ELSEVIER

Journal of Nuclear Materials 277 (2000) 280–287

journal of nuclear materials

www.elsevier.nl/locate/jnucmat

Irradiation-induced structural changes in surveillance material of VVER 440-type weld metal

M. Grosse[a], V. Denner[b], J. Böhmert[a,*], M.-H. Mathon[b]

[a] *Forschungszentrum Rossendorf, P.O. Box 510 119, D-01314 Dresden, Germany*
[b] *Laboratoire Léon Brillouin, CEA Saclay, 91191 Gif-sur-Yvette cedex, France*

Received 4 January 1999; accepted 29 June 1999

Abstract

The irradiation-induced microstructural changes in surveillance materials of the VVER 440-type weld metal Sv-10KhMFT were investigated by small angle neutron scattering (SANS) and anomalous small angle X-ray scattering (SAXS). Due to the high fluence, a strong effect was found in the SANS experiment. No significant effect of the irradiation is detected by SAXS. The reason for this discrepancy is the different scattering contrast of irradiation-induced defects for neutrons and X-rays. An analysis of the SAXS shows that the scattering intensity is mainly caused by vanadium-containing (VC) precipitates and grain boundaries. Both types of scattering defects are hardly changed by irradiation. Neutron irradiation rather produces additional scattering defects of a few nanometers in size. Assuming these defects are clusters containing copper and other foreign atoms with a composition according to results of atom probe field ion microscopy (APFIM) investigations, both the high SANS and the low SAXS effect can be explained.

1. Introduction

The weld joint of a reactor pressure vessel is considered as the potentially weakest link to its reliability [1]. This is not only because the weld presents a possible region of metallurgical discontinuities but also because the weld metal exhibits the highest sensitivity against neutron embrittlement. Although numerous studies have been concerned with the irradiation behaviour of weld metal, the reason for the high radiation sensitivity has not yet been understood.

Progress in our understanding can only be achieved by comprehensive microstructural investigations combining several methods of modern structure analysis. Microscopic methods like analytical high resolution transmission electron microscopy (TEM) or atom probe field ion microscopy (APFIM) provide information about single objects. Applying APFIM, an increase of the phosphorus grain boundary segregations and both copper- and phosphorus-enriched precipitates were detected in weld metals after neutron irradiation [2]. Copper-containing clusters were found by APFIM in neutron irradiated base metal [3]. Their chemical composition was 3.5% Si, 4% Ni, 1.5% Cu and 4% Mn, the balance to 100% is Fe. Similar clusters were also observed by APFIM in VVER 440-type base metal [4]. Due to the heterogeneity of the material, it is difficult to prove that such singular results are representative for the whole.

Small angle neutron or X-ray scattering (SANS, SAXS) gives integrative results but the information is only indirect and ambiguous. A sophisticated analysis of such experiments can, however, provide additional information about the type and composition of irradiation defects. With SANS, irradiation-induced inhomogeneities with a mean diameter between 2 and 4 nm, depending on the irradiation temperature but not on the damage dose, were found in Western weld metal [5]. The ratio (A-ratio) of the scattering intensity of this object measured perpendicular and parallel to the external magnetic field was between 3.5 and 2.0. In former own investigations at a laboratory heat of the VVER 440-type base metal (Russian notation 15Kh2MFA) vanadium-containing (VC) precipitates could be detected.

* Corresponding author. Tel.: +49-351 260 3186; fax: +49-351 260 2205.

0022-3115/00/$ - see front matter
PII: S0022-3115(99)00157-9

The volume fraction of these precipitates was higher in the irradiated state than in the unirradiated state [6].

The following study concerns SANS and SAXS experiments at VVER 440-type weld metal (Russian notation Sv-10KhMFT) irradiated to high fluences. Using the method of contrast variation in a very extended sense (comparison SANS–SAXS, SAXS by different X-ray energies, relation between nuclear and magnetic SANS), the study is to gain more detailed information on the microstructure of irradiated VVER 440-type weld metal.

2. Theoretical background of contrast variation in SANS and SAXS experiments

The differential macroscopic scattering cross-section $d\Sigma(Q)/d\Omega$, which is calculated from the measured small angle scattering intensity by the correction of the influence of the experimental conditions, is given by [7]

$$\left(\frac{d\Sigma(Q)}{d\Omega}\right) = k\int_0^\infty D_v(R)R^3\Delta\eta^2(R)\Phi(Q,R)\ dR, \tag{1}$$

Q is the value of the scattering vector, k a constant depending on the shape of the inhomogeneities and R their characteristic dimension. D_v is the volume distribution function of the inhomogeneities. $\Delta\eta^2$ characterizes the scattering contrast of the whole system consisting of matrix and inhomogeneities. The scattering density η is given by

$$\eta = nb, \tag{2}$$

n is the mean number density of the atoms or isotopes and b their mean scattering lengths. $\Delta\eta$ is the difference between the scattering densities of matrix and inhomogeneities. It depends only on the type of inhomogeneities for a given matrix. Therefore, a variation of η provides additional information about the structure and chemical composition of the objects seen by the small angle scattering.The so-called shape factor $\Phi(Q, R)$ is the Fourier transform of the shape of the inhomogeneities. For spheres $\Phi(Q, R)$ is given by

$$\Phi(Q,R) = \left(3\frac{\sin(QR) - QR\cos(QR)}{Q^3R^3}\right)^2. \tag{3}$$

By applying SANS to material systems with ferromagnetic components, the variation between the magnetic and nuclear scattering contrast can be used. The A-ratio, which is the ratio of the intensity $I(Q)_\perp$ perpendicular to the external magnetic field to the intensity $I(Q)_\parallel$ parallel to it, is given by

$$A = \frac{I(Q)_\perp}{I(Q)_\parallel} = \frac{\left(\frac{d\Sigma(Q)_{nuc}}{d\Omega}\right) + \left(\frac{d\Sigma(Q)_{mag}}{d\Omega}\right)}{\left(\frac{d\Sigma(Q)_{nuc}}{d\Omega}\right)} \tag{4}$$

and describes this contrast relation. $d\Sigma(Q)_{nuc}/d\Omega$ and $d\Sigma(Q)_{mag}/d\Omega$ are the nuclear and magnetic differential scattering cross sections.

SAXS experiments allow to use resonant scattering effects at energies close to the energies of the X-ray absorption edges of elements that are contained in the system. Here it is usual to make use of the multiplier of the Compton scattering length f, called atomic form factor, instead of the total scattering length. For small Q, the dependence of f on the X-ray energy can be calculated by

$$\lim_{Q\to 0} f = Z + f' + if'', \tag{5}$$

Z is the atomic number, f' and f'' are real and imaginary part of the resonant scattering contribution. The values of f' and f'' are significantly high only near the X-ray absorption edge. They can be calculated by the well-known Kramers–Kronig [8,9] and Cromer–Liberman [10] relations. According to Eq. (2) η is given by

$$\eta = nf. \tag{6}$$

3. Materials and measurements

The materials investigated were prepared from broken Charpy-V specimens which came from the embrittlement surveillance programme of two VVER 440 nuclear power plants [11]. They were irradiated to two fluences F_1 and F_2. In Table 1 the irradiation conditions are summarized. According to Russian standards the neutron flux ϕ and fluence $F = \phi t$ are given for $E > 0.5$ MeV.

The chemical composition is (in wt%): 0.05 C, 0.4 Si, 0.014 S, 0.028 P, 0.19 V, 1.30 Cr, 1.24 Mn, 0.18 Cu, 0.12 Ni, 0.43 Mo and balance Fe.

Fig. 1 shows the metallographic microstructure of the material. The microstructure exhibits the as-solidified structure. It is characterized by cellular columnar aligned prior austenite grains and contains pro-eutectoid ferrite at the prior austenite grain boundaries and tempered bainite inside the prior austenite grains.

TEM investigations were performed at 'Max-Planck-Institut für Metallforschung', Stuttgart. Fig. 2 shows a TEM photograph of the F_2-irradiated state. Additional to the carbide precipitates, which can also be found in the unirradiated state (larger black dots), numerous fine precipitates (small black dots) appear. The black dots are heterogeneously distributed. The larger ones (vanadium carbides) are concentrated near dislocations.

The SANS experiments were performed at Laboratoire Leon Brillouin (CEA-CNRS Saclay, France) at the PAXE facility. For that, samples were cut from Charpy-V specimens as slices of 0.8 mm. During the

Table 1
Irradiation conditions of the material investigated

Code	Reactor	Irradiation temperature (°C)	Neutron flux ϕ (10^{16} m^{-2} s^{-1}) ($E>0.5$ MeV)	Neutron fluence $F=\phi t$ (10^{24} m^{-2}) ($E>0.5$ MeV)
F_1	Rovno unit 1 (VVER 440-V 213), reduced core	270	0.36	0.62
F_2	Armenia unit 2 (VVER 440–230), full core	270	3.2	6.3

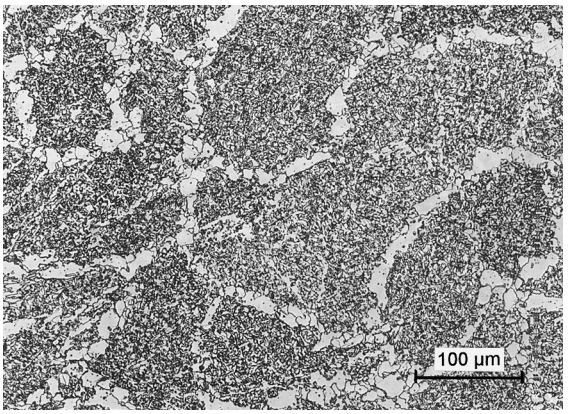

Fig. 1. Metallographic microstructure of the VVER 440-type weld metal Sv 10KhMFT.

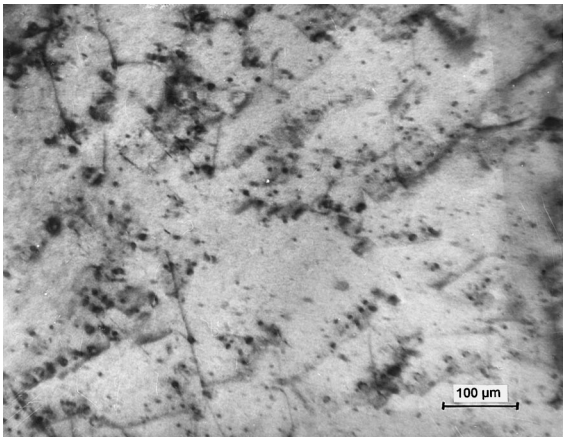

Fig. 2. TEM photograph of the F_2-irradiation state of the weld metal Sv-10KhMFT.

measurements, the samples were subjected to a 1.4 T magnetic field perpendicular to the incident beam. Such a magnetic field leads to saturation magnetization of the samples [12]. Two configurations with wavelengths of 0.5 and 0.6 nm and sample to detector distances of 1.5 and 5 m, respectively, were applied to get a Q-range of 0.085 to 2.42 nm^{-1}. Software from LLB Saclay was applied for the initial data analysis. For absolute calibration the direct beam method [13] was used. As the scattering intensity shows a constant (e.g., Q independent) scattering contribution, the data had to be corrected. Therefore, this contribution was estimated with the method given in [14] by using the asympthotic scattering behaviour at large Q values. In this way the macroscopic differential scattering cross section $d\Sigma(Q)/d\Omega$ was determined. From that the size distribution function was calculated by the programme ITP92 developed by Glatter [7].

For the SAXS experiments slices were cut from the same Charpy-V specimens. The thickness of the slices was reduced to about 15 µm by mechanical grinding and mechanical and following mechano-chemical polishing. The SAXS measurements were performed at the JUSIFA facility at HASYLAB (DESY Hamburg, Germany). An overview energy scan was performed at energies close to the V-, Cr-, Mn- and Fe–K-absorption edge using equidistant steps of f'. Additionally, the SAXS intensity was measured at two energies close to the absorption edge of vanadium (5466 and 5536 eV) with a high measurement time (very high number of counts) in order to decrease the data scattering caused by the counting statistics. Due to the Fe fluorescence radiation, SAXS measurements at energies higher than the energy of the Fe–K-absorption edge are not possible.

4. Results

The estimated values for the constant scattering contribution and the Porod constants are given in Table 2. In contrast to the results in [14] no systematic variation of the constant scattering contribution with irradiation was found for the investigated material. The Porod constant, which is proportional to the specific surface of the scattering inhomogeneities, is significantly raised after neutron irradiation. It shows that the mean specific surface of the irradiation-induced defects is higher than that of the inhomogeneities existing in the unirradiated state.

Fig. 3(a) and (b) show the differential neutron scattering cross sections $d\Sigma(Q)/d\Omega$ of the unirradiated and the two irradiated states parallel and perpendicular to the external magnetic field, respectively. The shape of the Q dependence of $d\Sigma(Q)/d\Omega$ does not depend on the angle to the magnetic field, which proves that the chemical and the magnetic inhomogeneities are identical. A strong irradiation effect is found at higher Q whereas the low Q

Table 2
Constant scattering contribution and Porod constant for the investigated irradiated states

	Constant scattering contribution (10^{-3} cm^{-1})		Porod constant (10^{-9} nm $^{-5}$)	
	Magnetic	Nuclear	Magnetic	Nuclear
Unirradiated	0.59 ± 0.14	2.58 ± 0.13	0.5 ± 0.4	1.3 ± 0.4
Irradiated, *F*1	1.40 ±0.26	2.87 ± 0.12	4.1 ± 0.4	3.1 ± 0.3
Irradiated, *F*2	1.01 ±0.29	1.96 ± 0.13	4.1 ± 1.1	10.7 ± 0.4

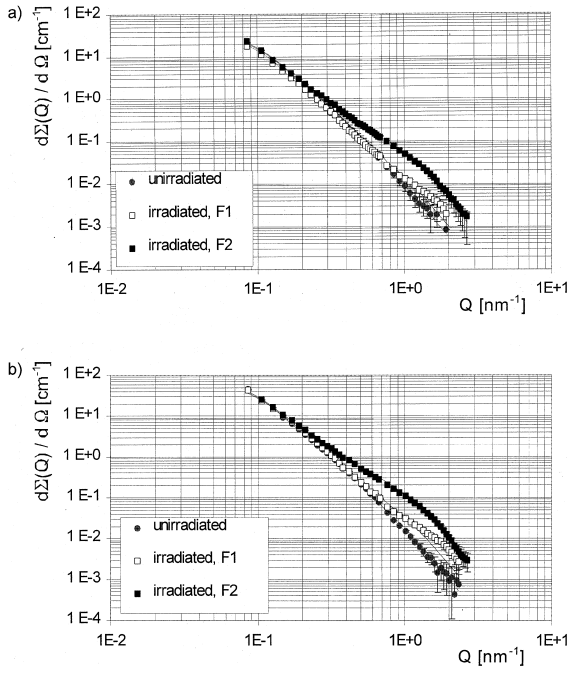

Fig. 3. Differential neutron scattering cross section $d\Sigma(Q)/d\Omega$ of the unirradiated and the two irradiated states of weld metal Sv-10MFT, (a) parallel and (b) perpendicular to the external magnetic field as a function of the scattering vector.

region is hardly influenced by the irradiation. The *A*-ratios for the irradiated states are given in dependence on Q in Fig. 4. In the unirradiated state a weak decrease with increasing Q from 2.0 to 1.8 at $Q = 1.2$ nm^{-1} is found. At higher Q-value the scattering of A is very high. However, the *A*-ratio seems to decrease up to a level of about 1. For the irradiated states the *A*-ratio is fairly constant at about 2.0 and does not depend on the fluence.

Assuming the irradiation-induced defects are non-ferromagnetic, what is probably realistic for the irradiation defects, the magnetic scattering contrast is known

$$\Delta\eta^2_{\text{magn}} = \eta^2_{\text{magn}_{\text{Fe}}}, \tag{7}$$

$\eta_{\text{magn}_{\text{Fe}}}$ is the magnetic scattering length density of iron.

Thus, absolute size distribution functions related to the volume fraction of the defects can be calculated. The

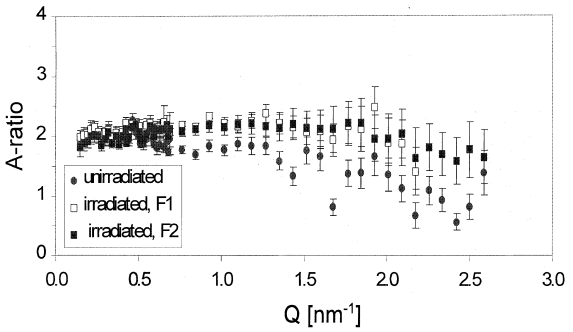

Fig. 4. Dependence of the *A*-ratio on the scattering vector Q.

size distributions derived from the difference between scattering perpendicular and parallel to the magnetic field (magnetic SANS intensity) are depicted in Fig. 5 for the three material states.

In the unirradiated state the distribution curve is flat and has a weakly extended maximum at about 5 nm.

Neutron irradiation produces defects in the size range between 0.5 and 4.5 nm. The size distribution function has a maximum at about 2.0 nm. The full width at half maximum is about 1.6 nm. The shape of the peak and the position of the maximum do not depend on the fluence, whereas the volume fraction of the irradiation-induced defects clearly increases with the fluence. The formation of tiny inhomogeneities results in an increase of their specific surface. It is confirmed by the estimated Porod constants.

Fig. 6 shows the SAXS intensity of the material in the unirradiated state and in the state irradiated to the higher fluence F_2. Contrary to the SANS data, no irradiation-induced increase of the SAXS intensity was found. Surprisingly, the SAXS intensity of the unirradiated state is even slightly higher than in the irradiated state, at least in the Q-range close to 0.5 nm^{-1}. This is clear to see in Fig. 7 where the integral intensity in the Q-range of $0.5 \leqslant Q \leqslant 1$ nm^{-1} is shown in dependence on the X-ray energy. The integral intensity is almost constant within the investigated energy range. Only small contrast variation appears near the K_α-X-ray absorption edge of vanadium for both the unirradiated state and the irradiated state. A rather small variation was measured at the K_α-X-ray absorption edge of manganese in the unirradiated state. The steep decrease of the SAXS

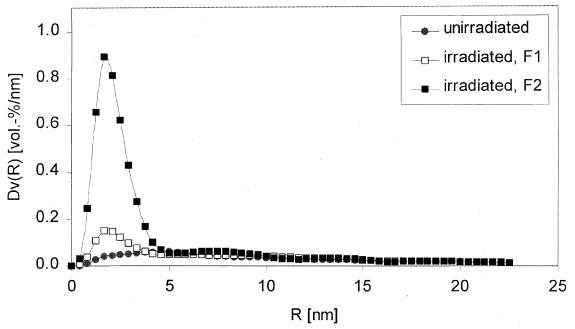

Fig. 5. Particle size distribution of the investigated material states.

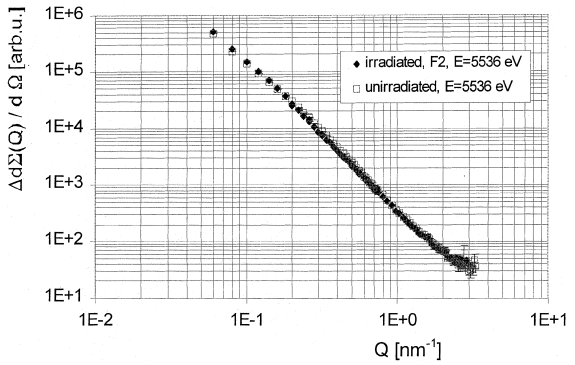

Fig. 6. SAXS cross section of the unirradiated and irradiated (F_2) state measured with an X-ray energy of 5536 eV.

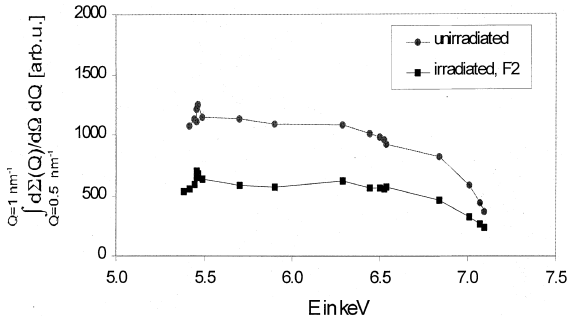

Fig. 7. Dependence of the integral SAXS cross section in the range of $0.5 \leqslant Q \leqslant 1.0$ nm^{-1} on the X-ray energy.

intensity close to the iron K_α-absorption edge follows approximately the decrease of the square of the mean scattering length density of the matrix as expected.

The SAXS intensity diminishes proportional to $Q^{-2.5}$ for both the unirradiated and irradiated states (Fig. 6). An exponent of -2.5 is not typical for compact objects but it is comparable with the theoretical value of -2.0 derived for thin discs or spherical shells [15]. This could imply that the SAXS is dominated by the scattering of grain boundaries which are seen as thin discs or shells by the X-rays. An analysis of the azimuthal intensity distribution confirms this interpretation.

In this case the higher intensity of the unirradiated state would be caused by a stronger grain boundary scattering.

The TEM investigation reveals the existence of vanadium carbides of a diameter of smaller than 10 nm in both the unirradiated state and after irradiation. In order to get information about the irradiation behaviour of the VC precipitates the contrast variation at X-ray energies near the energy of the vanadium absorption edge was applied. The difference of the scattering cross section $\Delta[\mathrm{d}\Sigma(Q)/\mathrm{d}\Omega]$ between the differential SAXS cross section measured at X-ray energies of 5466 and 5536 eV was analysed for the unirradiated state and the state irradiated to the fluence F_2. It only depends on the variation of the scattering contrast. Taking into account Eqs. (1),(5),(6) this difference is proportional to

$$\begin{aligned}\frac{\mathrm{d}\Sigma(Q,E_1)}{\mathrm{d}\Omega} - \frac{\mathrm{d}\sum(Q,E_2)}{\mathrm{d}\Omega} &\sim \Delta\eta(E_1)^2 - \Delta\eta(E_2)^2 \\ &\sim n_\mathrm{P}^2[\langle Z+f'\rangle_\mathrm{P}^2(E_1) \\ &\quad - \langle Z+f'\rangle_\mathrm{P}^2(E_2)] - 2n_\mathrm{P}n_\mathrm{M}\langle Z+f'\rangle_\mathrm{M} \\ &\quad \times [\langle Z+f'\rangle_\mathrm{P}(E_1) - \langle Z+f'\rangle_\mathrm{P}(E_2)] \\ &\quad - n_\mathrm{P}^2[f_\mathrm{P}''^2(E_1) - f_\mathrm{P}''^2(E_2)] + 2n_\mathrm{P}n_\mathrm{M}f_\mathrm{M}'' \\ &\quad \times [f_\mathrm{P}''(E_1) - f_\mathrm{P}''(E_2)], \end{aligned} \tag{8}$$

$n_{\mathrm{P,M}}$ are the mean number densities of the particles or matrix, respectively, and $f_{\mathrm{P,M}}$ are their mean atomic form factors. An impression of the influence of the different alloy elements on the difference effect provides Table 3 where the real $(Z+f')$ and imaginary (f'') part of the atomic form factor are made up for the most important elements in the material and the mean value of the matrix for the two energies together with their differences and the differences of their squares. It can be seen that the difference between the scattering at the two energies is mainly caused by the differences in the square of the atomic form factor of vanadium. Therefore, this difference in the differential scattering cross sections gives information mainly about VC inhomogeneities. Fig. 8 compares $\Delta[\mathrm{d}\Sigma(Q)/\mathrm{d}\Omega]$ between the two energies of the unirradiated with that of the as-irradiated (F_2) state. In the Q-range, in which the strong irradiation effect was found in the SANS experiment, the vanadium-effected scattering of the unirradiated and irradiated state does not differ significantly. This proves that the irradiation-induced defects do not contain significant amounts of vanadium in this weld metal. At low Q-values the SAXS cross section is higher for the irradiated than for the unirradiated state whereas the unirradiated state has a higher cross section in the middle range of Q.

Table 3
Parameters to characterize the scattering contrast near the vanadium absorption edge in SAXS experiments

E (eV)		C	Si	V	Cr	Mn	Fe	Mo	Matrix
$E_1 = 5466$	$(Z + f')$	6.03	14.35	14.25	21.75	23.32	24.63	41.9	24.47
	f''	0.03	0.68	4	0.54	0.64	0.75	5.27	0.76
$E_2 = 5536$	$(Z + f')$	6.03	14.35	19	21.73	23.26	24.6	42	24.45
	f''	0.03	0.66	3.9	0.54	0.62	0.73	5.16	0.74
E_1–E_2	$\Delta(Z + f')$	0	0	−4.75	0.02	0.06	0.03	0	0.02
	$\Delta(f'')$	0	0.02	0.1	0	0.02	0.02	0.11	0.02
	$\Delta(Z + f')^2$	0	0	−158	0.87	2.79	1.48	−0.8	0.98
	$\Delta(f'')^2$	0	0	0.79	0	0	0.03	1.15	0.03

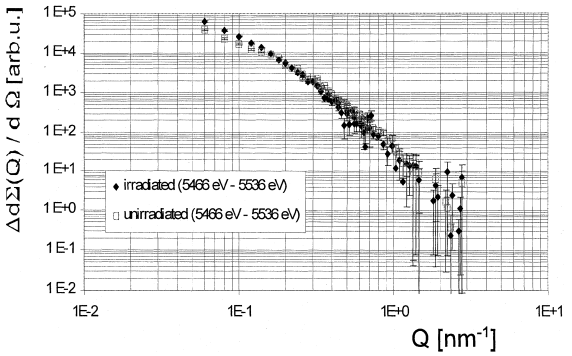

Fig. 8. Difference of the SAXS cross section of VC inhomogeneities measured by energies of 5466 and 5536 eV.

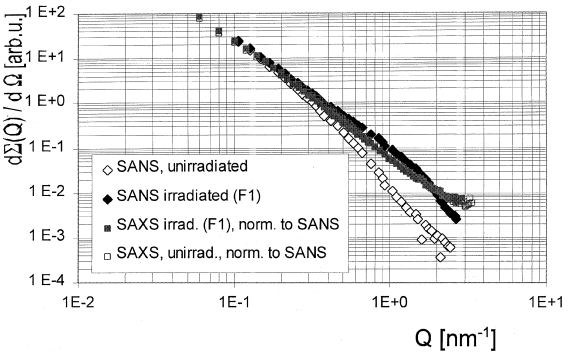

Fig. 9. Comparison between SANS cross section perpendicular to the magnetic field and SAXS cross section of the investigated material.

5. Discussion

Considering the scattering effects by SANS and SAXS as shown in Figs. 3 and 6, the different scattering response of neutrons and X-rays is obvious. For illustrating this once more the SANS cross section perpendicular to the magnetic field and SAXS cross section is compared for the unirradiated and an irradiated (F_2) state in Fig. 9. To make it clearer the SAXS cross section is normalized to the SANS cross section. As irradiation does not change the SANS cross section at low Q-values, the normalization is performed so that SANS and SAXS cross sections have approximately the same value in the low Q-range.

The following insights can be extracted from this comparison:

- Irradiation-induced defects exhibit a much stronger scattering contrast for neutrons than for X-rays.
- There are defects in the unirradiated state with a higher scattering contrast for X-rays than for neutrons, but these defects are hardly influenced by the irradiation.

In Fig. 10 the comparison is specially focused on the VC inhomogeneities. Therefore, the SANS cross section is compared with the difference of the SAXS cross section measured at X-ray energies of 5466 and 5536 eV. This difference is also normalized to the SANS cross section at low Q-values. A good agreement can be found between the shape of the SAXS cross section of the VC inhomogeneities and the shape of the SANS cross section of the unirradiated state. This proves that in the unirradiated state SANS is mainly caused by VC inhomogeneities.

To understand the experimental results a system of three types of scattering inhomogeneities is presumed. It consists of

- vanadium carbides V_xC_y,
- grain boundaries,
- clusters containing copper, manganese, silicon, nickel and phosphorus.

Dislocations, which also exist in the material, can be neglected. Calculations with dislocation densities which were determined by TEM in similar material have shown, that their scattering contribution is lower by about two orders of magnitude than the scattering of the vanadium carbides [16]. Chromium-rich $M_{23}C_6$ or M_7C_3 precipitates can also be detected by TEM but they are too large (200–1000 nm) to give a significant scattering contribution in the measured Q-range.

The scattering contrast for the three above-mentioned inhomogeneities is calculated and compared in Fig. 11 where the scattering contrast is normalized to the scattering contrast of grain boundaries. For the

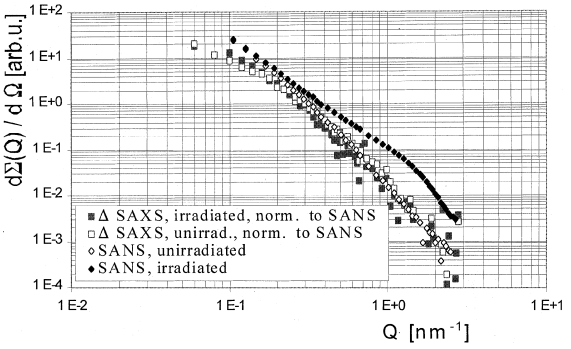

Fig. 10. Comparison between the SANS cross section perpendicular to the magnetic field and the difference of the SAXS cross section measured by energies of 5466 and 5536 eV.

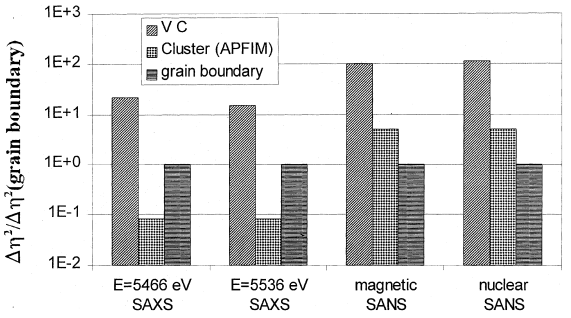

Fig. 11. Comparison of the contrast for magnetic and nuclear neutron scattering and for X-ray scattering at energies of 5466 and 5536 eV of vanadium carbides, grain boundaries and clusters detected by APFIM [4].

clusters a composition is assumed corresponding to APFIM results of VVER 440-type base metal [4]. Furthermore, an unchanged number density like the matrix is supposed. It can be seen that in this system the grain boundaries are much better visible for X-rays than for neutrons. The ratio of the scattering contrast of grain boundaries to the scattering contrast of vanadium carbides is nearly one order of magnitude higher for X-rays than for neutrons. Contrary, the copper containing clusters which were detected by APFIM are much better visible for neutrons than for X-rays. The ratio of the scattering contrast of these clusters to the scattering contrast of vanadium carbides is more than one order of magnitude higher and the ratio to the scattering contrast of grain boundaries nearly two orders of magnitude higher for neutrons than for X-rays.

In the unirradiated state the scattering is caused by vanadium carbides and grain boundaries. Due to the different contrast ratios the SAXS intensity at high Q-values is mainly caused by grain boundary scattering whereas the SANS intensity is dominated by the scattering at the vanadium carbides. The theoretical A-ratio for pure vanadium carbides is between 1.8 and 2.0 depending on the stoichiometric relations and structure type. For grain boundaries the A-ratio is 1.4. The experimentally measured A-ratios between 1.8 and 2.0 agree with the expected values for the dominating VC-precipitates. The higher grain boundary SAXS effect of the unirradiated state compared to that of the irradiated one (Fig. 7) is not obviously understood. As a reason the heterogeneity of the microstructure of the weld metal cannot be excluded. Another possibility to explain this effect could be the grain boundary trapping of small foreign atoms (for instance P), which becomes mobile by the irradiation. This trapping can compensate, at least partially, the difference in the number density of iron atoms between grain boundaries and matrix. This would reduce the scattering contrast of the grain boundaries to the matrix.

Irradiation results in the formation of clusters. These clusters are not really visible for X-rays but detectable by neutrons. This explains why the SAXS intensity is not increased by irradiation whereas SANS provides a strong increase of the intensity. Due to the high iron content in the cluster (about 80%) it cannot be excluded that these kinds of defects be ferromagnetic. Thus, the calibration of Fig. 5 is not longer absolute. However, the principle shape of the size distribution function is not influenced by this fact. As both the number density and the chemical composition of clusters are not certainly known, the absolute calibration and the A-ratio of clusters cannot be calculated. Assuming the same number density as in the iron matrix, a chemical composition given in [4] and the identity of the magnetic moment of the iron atoms in the clusters and in the matrix, the A-ratio amounts to about 2.0. Taking into account a content of vacancies between 0 and 12% and considering the standard deviation of the content of foreign atoms in the clusters, the A-ratio would range between 1.6 and 3.5. Thus, the assumption that the irradiation-induced precipitates are copper-containing clusters is not contradicting to the A-ratio experimentally estimated for the investigated material.

6. Conclusion

SANS and SAXS experiments were performed to recognize type and characteristic of the irradiation-induced defects in the VVER 440-type weld metal Sv-10MFT. Their results were compared with results from TEM and APFIM investigations. Neglecting dislocations and large chromium-rich carbides, whose scattering contribution is very weak in the measured Q-range, three types of inhomogeneities are detected by the small angle scattering experiments:

- vanadium carbides V_x C_y,
- grain boundaries and
- clusters containing copper, manganese, silicon, nickel and phosphorus [4]

These three types of defects result in different scattering contrasts if one compares SANS and SAXS as well as SAXS at different energies closely above and below the X-ray K-absorption edge of vanadium or the magnetic and nuclear SANS contributions.

Grain boundary scattering and the scattering at the vanadium carbides are observed. In the irradiated state an additional scattering contribution can be observed by SANS but not by SAXS. Assuming the irradiation-induced scattering is caused by clusters of a type that was identified by APFIM as an irradiation defect, all measured contrast variation effects can be explained.

These results should be verified by thermodynamic investigations using the annealing behaviour of the irradiation defects. APFIM investigation at the same material would be helpful to confirm the results.

Acknowledgements

The authors thank Mr G. Goerigk from Forschungszentrum Jülich for supporting measurements and helpful discussions of the results. Thanks are expressed to Mr Kopold from Max-Planck-Institut für Metallforschung for performing the TEM investigations.

References

[1] L.E. Steele, Neutron irradiation embrittlement of reactor pressure vessel steels, IAEA, Technical Prints Series, No. 163, Vienna, 1975.
[2] M.K. Miller, T. Jayaram, K.F. Russel, J. Nucl. Mater 225 (1995) 215.
[3] S.Miloudi, private communication.
[4] A. Kruykov, Workshop on Composition Effects on Neutron Embrittlement, Rossendorf, 1998.
[5] J.T. Buswell, P.J.E. Bischler, S.T. Fenton, A.E. Word, W.J. Phythian, J. Nucl. Mater 205 (1993) 198.
[6] M. Große, F. Eichhorn, J. Böhmert, G. Brauer, H.-G. Haubold, Nucl. Instrum. Methods B 97 (1995) 487.
[7] O. Glatter, J. Appl. Crystallogr. 13 (1980) 7.
[8] H.A. Kramer, Phys. Z. 30 (1929) 522.
[9] R. de L. Kronig, J. Opt. Soc. Am. 12 (1926) 547.
[10] D.T. Cromer, D. Liberman, J. Chem. Phys. 53 (1970) 1891.
[11] A.D. Amayev, A.M. Kryukov, M.A. Sokolov: Irradiation embrittlement of VVER 440 vessel materials estimated by the surveillance specimen test, in: S.B. Trudov (Ed.), Nauchnykh IAE I.V.Kurtchatova, Kurtchatov Institute of Atomic Energy, Moscow 1989, pp 16–23.
[12] G. Brauer, F. Eichhorn, F. Frisius, R. Kampmann, in: A.S. Kumar, D.S. Gelles, R.K. Nanstad (Eds.), Effects of Radiation on Materials, Proceedings of the 16th International Symposium, ASTM-STP 1175, American Society for Testing and Materials, Philadelphia, 1993, p. 346.
[13] J.P. Cotton, in: P. Lindner, Th. Zemb (Eds.), Neutron, X-ray and Light Scattering, North Holland, Elsevier, Amsterdam, 1991, p. 19.
[14] M. Grosse, J. Boehmert, R. Gilles, J. Nucl. Mater. 254 (1998) 143.
[15] H.-G. Haubold, Röntgenkleinwinkelstreuung an Synchrotronstrahlungsquellen, in 23. IFF-Fereinkurs Synchrotronstreuung zur Erforschung kondensierter Materie, ISBN 3-89336-088-3 Forschungszentrum Jülich, 1992, 19.1.
[16] A.Gokhman, private communication.